Thermodynamic analysis of an improved integrated biomass gasifier solid oxide fuel cell micro combined heat and power system

Cavalli, A.; Monteiro Fernandes, A.B.; Aravind, P. V.

DOI
10.1016/j.energy.2021.120945

Publication date
2021

Document Version
Final published version

Published in
Energy

Citation (APA)
Cavalli, A., Monteiro Fernandes, A. B., & Aravind, P. V. (2021). Thermodynamic analysis of an improved integrated biomass gasifier solid oxide fuel cell micro combined heat and power system. *Energy*, *231*, Article 120945. https://doi.org/10.1016/j.energy.2021.120945

Energy 231 (2021) 120945

Contents lists available at ScienceDirect

Energy

journal homepage: www.elsevier.com/locate/energy

Thermodynamic analysis of an improved integrated biomass gasifier solid oxide fuel cell micro combined heat and power system

A. Cavalli*, A. Fernandes, P.V. Aravind

Process & Energy Department, 3me Faculty, Delft University of Technology, Leeghwaterstraat 39, 2628 CB, Delft, the Netherlands

ARTICLE INFO

Article history:
Received 7 January 2020
Received in revised form
8 May 2021
Accepted 13 May 2021
Available online 15 May 2021

Keywords:
Biomass gasifier
Solid oxide fuel cell
Direct internal tar reforming
High temperature gas cleaning
Thermodynamic analysis

ABSTRACT

Limited overall efficiency and excessive complexity can hinder the competitiveness of biomass gasifier solid oxide fuel cell micro combined heat and power systems. To overcome these problems, hydrocarbons direct internal reforming is analysed as a strategy to increase efficiency and reduce system complexity. To the same end, two biosyngas heating-up strategies are compared: catalytic partial oxidation and afterburner off gases utilization. A comprehensive approach combining thermodynamic equilibrium calculations, experimental measurements, and system modelling was used. The gas cleaning unit should operate at 400 °C to decrease H_2S and HCl below 1 ppmv. A tar amount of 120–130 g Nm^{-3} dry biosyngas for woodchips and 190 g Nm^{-3} for straw pellets was measured and 2-methoxyphenol, hydroxyacetic acid and hydroxyacetone were selected as representative compounds. With direct internal reforming the cathode air flow rate decreases from approximately 90 kg h^{-1} to 60 kg h^{-1}. This leads to an increase of around 1% point in electrical efficiency and of even 5–6% points in thermal efficiency. Direct internal tar reforming seems therefore an advantageous strategy. The catalytic partial oxidation unit increases the system overall efficiency but reduces the electric efficiency from roughly 38%–30% and is therefore not advised.

1. Introduction

Combining biomass gasification with high temperature fuel cells has received considerable attention as an alternative to fossil fuel based energy systems [1–4]. In a biomass gasifier solid oxide fuel cell (SOFC) system, the biomass is converted into biosyngas, a mixture of hydrogen, carbon monoxide, carbon dioxide, nitrogen, and methane, which is converted into heat and electricity in the SOFC. Biosyngas also contains minor compounds which are harmful for downstream equipment and have to be removed: sulphur, halides, particulate matter and tar compounds [5]. The biosyngas composition and the content of tar are highly dependent on the gasification agent used, that can be air, oxygen, or steam [6]. Before entering the SOFC, the gas passes through a gas cleaning unit (GCU) where the contaminants are removed at low (<300 °C) or high temperature. Gas cleaning is a crucial step in the system heat management, and it strongly affects the complexity and overall system efficiency.

In literature, system modelling has been used to determine the obtainable electric and overall efficiencies with the different cleaning methods, and to optimize the design of biomass gasifier SOFC systems. Omosun et al. modelled two combined heat and power (CHP) systems: a downdraft gasifier with cold gas cleaning, obtaining an efficiency of 20.8% electrical and 33.9% overall, and a fluidized bed gasifier with hot gas cleaning, achieving an efficiency of 22.6% electrical and 59.6% overall [7]. Aravind et al. evaluated the performance of a 100 kW gasifier SOFC system with a gas turbine (GT) bottoming cycle. With gas cleaning at 750 °C, the system achieved 54% electrical and 77–78% total efficiency, whereas cleaning the gas at ambient temperature resulted in 49.5% electrical and 49.9–57% total efficiency [8]. Toonssen et al. investigated the performance of a 30 MW_e integrated gasifier hybrid SOFC-GT systems. Cleaning the gas at 700 °C instead of 120 °C gave an increase in the exergy efficiency of only 0.5% [9]. Liu et al. found that cleaning the gas at 450 °C gave a CHP energy efficiency of 65%, while cleaning the gas at ambient temperature lowered the efficiency to 57% [10]. More recently, Doherty et al. found that in a 120 kW_e dual fluidized bed steam gasifier SOFC system, increasing the cleaning temperature from 400 °C to 700 °C increased the system net electrical efficiency from 25.3% to 30.2% but decreased the CHP

* Corresponding author.
E-mail address: a.cavalli@tudelft.nl (A. Cavalli).

https://doi.org/10.1016/j.energy.2021.120945
0360-5442/

Nomenclature

Acronyms

AC	Alternating Current
ASR	Area Specific Resistance
CFD	Computational Fluid Dynamics
CHP	Combined Heat and Power
CPOX	Catalytic Partial Oxidation
DC	Direct Current
EUBCE	European Biomass Conference and Exhibition
FT-IR	Fourier-Transform Infrared Spectroscopy
GC-MS	Gas Chromatography Mass Spectrometry
GCU	Gas Cleaning Unit
IGCC	Integrated Gasification Combined Cycle
LHV	Lower Heating Value
SOFC	Solid Oxide Fuel Cell

Symbols

E_{rev}	Reversible voltage
F	Faraday constant
h	Enthalpy
j	Current density
$\dot{m}$	Mass flow rate
$P_{O_{2,cathode}}$	Equilibrium oxygen partial pressure at cathode
$P_{O_{2,anode}}$	Equilibrium oxygen partial pressure at anode
$\dot{Q}$	Heat flow
R	Universal gas constant
T	Temperature
V	Voltage
$\dot{W}$	Power
Δ	Variation
η	Efficiency

efficiency from 69.5% to 67.0% [11]. Several recent works in the literature discuss other important aspects of biomass gasifier solid oxide fuel cell systems, or their integration with additional bottoming cycles [12–15].

Among biosyngas contaminants, tar, together with light condensable and volatile organic compounds, require particular attention. These compounds can condense in cold spots and cause carbon deposition in downstream equipment. However, they are hydrocarbons and could be regarded as useful fuel. In low temperature GCUs, tar, light condensable and part of the volatile organic compounds are removed from the gas. Differently, in high temperature GCUs, these compounds are converted into H_2 and CO by reforming in a dedicated reactor via the endothermic reactions (1–3) [16,17].

$$\text{Steam reforming: } C_xH_yO_z + (x - z)H_2O \rightarrow xCO + [(x + y/2 - z)]H_2 \quad (1)$$

$$C_nH_x\,(\text{tar}) + nH_2O \rightarrow (n + x/2)H_2 + nCO \quad (2)$$

$$\text{Dry reforming: } C_nH_x\,(\text{tar}) + nCO_2 \rightarrow (x/2)H_2 + 2nCO \quad (3)$$

The heat required for these reactions can be provided by the SOFC outlet gas, either via heat exchangers or anode recirculation, or by biosyngas partial oxidation. However, heat transfer limitations decrease the overall system efficiency, while partial oxidation and recirculation lower biosyngas reactant concentrations. Reforming might take place internally in the SOFC due to the presence of Ni catalyst and the high operating temperature. In internal reforming, the heat required is provided directly by the SOFC, and the reactions can take place in a separate chamber (indirect internal reforming) or in the anode chamber (direct internal reforming), as illustrated in Fig. 1. Internal reforming eliminates the need of an additional reactor in the GCU, and improves and simplifies the system heat management. Moreover, the endothermic reforming reactions can cool down the SOFC, thus decreasing the energy consumed by the cathode air blower and making the system more efficient.

Some studies have already analysed the advantages of internal CH_4 reforming in high temperature fuel cell systems. Lanzini et al. investigated the efficiency and economic gain obtainable by increasing syngas CH_4 content in an integrated coal gasifier SOFC system [18]. In a previous study, Nagel et al. compared seven 1 MW_e integrated biomass gasifier SOFC systems. Two configurations adopted internal CH_4 reforming and a methanation reactor to increase CH_4 amount in biosyngas [19,20]. Di Carlo et al. compared the efficiency of a molten carbonate fuel cell coupled with a fast internally circulated fluidized-bed biomass gasifier with internal or external methane reforming; the former increased the stack efficiency from 42% to 53% and reduced the cathode flow rate by 30% [21]. In the analysis of a 120 kW_e biomass gasifier SOFC and Stirling engine system, Rokni concluded that using a methanizer before the SOFC reduced the cathode air necessary for cooling, hence less SOFC outlet gas heat was necessary to preheat biosyngas, thus increasing the system electrical efficiency by 2% points [22]. While the benefits of CH_4 internal reforming have been investigated, little if any information is available on the advantages of direct internal reforming of other hydrocarbons (i.e., tar, light condensable and volatile organic compounds).

The competitiveness of biomass gasifier SOFC systems, especially at micro scale (<250 kW fuel input power), can be hindered by the limited overall system efficiency typical of low temperature gas cleaning units and by the complexity of both low and high temperature GCUs. To overcome these problems, within the "FlexiFuel-SOFC" project, TU Delft investigated the possibility to adopt new design strategies. In this work, we use a comprehensive approach combining thermodynamic equilibrium calculations, experimental measurements, and system modelling to evaluate the efficiency gain obtainable with direct internal reforming of hydrocarbons. Moreover, we compare two strategies to heat up the biosyngas leaving the GCU and entering the SOFC: a catalytic partial oxidation reactor where part of the biosyngas is combusted, and a heat exchanger where the SOFC afterburner off gases are used. The analysis covers two biomass feedstocks with different humidity content since this parameter affects significantly the biosyngas composition and the tar content. An updraft gasifier was selected based on a. the possibility to handle different types of biomass in terms of moisture and size, b. the low amounts of particulate matter in the biosyngas, c. the high gasification efficiency [23]. Furthermore, the high quantity of light condensable and volatile organic compounds and tar produced in an updraft gasifier (around 150 g Nm^{-3} dry basis [23]) presents an opportunity for direct internal tar reforming. The results of the study are expected to contribute to the development of micro scale biomass gasifier fuel cell systems.

2. System configuration

The system in analysis is being developed under the European

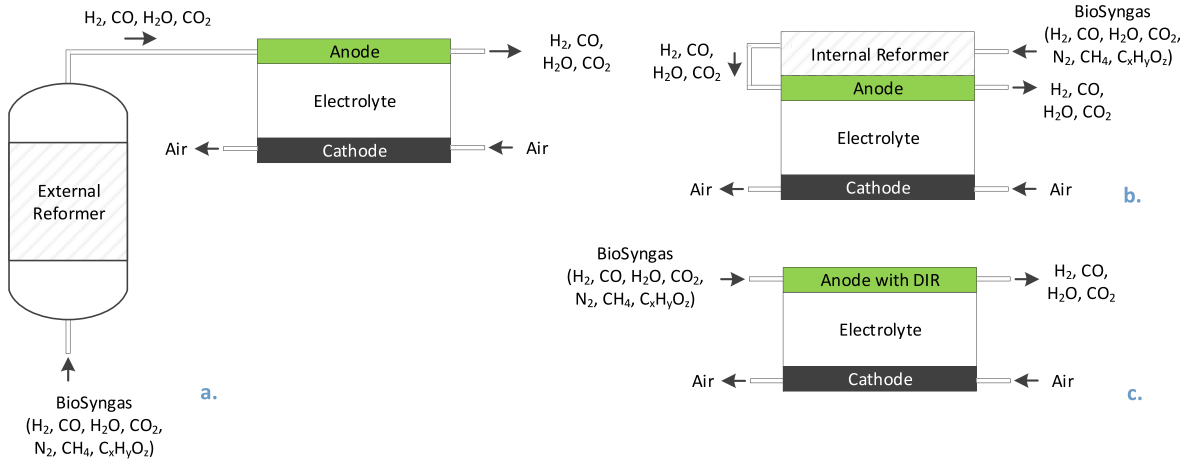

Fig. 1. Hydrocarbon reforming in SOFC systems: a. External Reforming, b. Indirect Internal Reforming, c. Direct Internal Reforming.

Union's Horizon 2020 project "FlexiFuel-SOFC". The system has three main components: a 50 kW_{th} (fuel input power) updraft biomass gasifier, a gas cleaning unit, and a 6 kW_e SOFC system. A fraction of the biosyngas is extracted from the gasifier in a slip stream and, after the contaminant removal stage, is fed to the SOFC. The focus of the study is on the SOFC system and on the gas cleaning step; therefore, the model does not include the gasifier, but it starts from the slip stream and ends with the boiler (part of the gasifier), where the SOFC afterburner off gases are used to generate heat together with the remaining biosyngas not extracted for electricity production. The gasifier (PuroWIN technology), including the burner and the boiler, was developed by WindHager in cooperation with the research institute BIOS Bioenergysysteme.

The GCU, developed by TU Delft and HyGEAR, has to provide biosyngas with a concentration of H_2S below 1 ppmv, HCl below 5 ppmv and particulate matter lower than 1 mg Nm^{-3}. These values were selected based on state-of-the-art knowledge of SOFC tolerance limits [24]. Two high temperature fixed bed reactors are used to clean the biosyngas from sulphur and chlorine and a ceramic filter for particulate matter removal. For what concerns tar, volatile organic and light condensable compounds reforming, and the heating up of the biosyngas between the GCU and the SOFC, four different configurations were analysed:

1. CASE A: External reforming - Heat in the afterburner off gases is used for the reforming reactions and to heat up the biosyngas entering the reformer.
2. CASE B: External reforming - Heat in the afterburner off gases is used for the reforming reactions. A catalytic partial oxidation (CPOX) reactor is used to heat up the biosyngas entering the reformer.
3. CASE C: Internal reforming – A CPOX reactor is used to heat up the biosyngas entering the SOFC.
4. CASE D: Internal reforming - Heat in the afterburner off gases is used to heat up the biosyngas entering the SOFC.

The SOFC stack system was developed by Fraunhofer IKTS and AVL. The system includes an afterburner where the residual fuel in the anode outlet gases is combusted with the cathode outlet air. In all the cases analysed, the cathode inlet air is pre-heated by the afterburner off gases.

3. Methodology

To evaluate the system efficiency gain obtainable with direct internal reforming and identify the most efficient biosyngas heating-up strategy, a comprehensive approach combining system modelling, thermodynamic equilibrium calculations and experimental data from the gasifier of the "FlexiFuel-SOFC" project was used. In this section, each activity is described in detail.

3.1. Thermodynamic equilibrium calculations

Thermodynamic equilibrium calculations were used first in the system conceptual design phase to compute the steam necessary to avoid carbon formation, and second to discover which sulphur and chlorine compounds can be expected in the biosyngas, thus helping with the selection of suitable sorbents. Finally, the calculations were used to determine the GCU operating temperature allowing to achieve the target cleaning values. The software FactSage v5.4.1 was used for the thermodynamic equilibrium calculations. Taking as inputs the mass of the reactants, process temperature, and pressure, the software gives as outputs the products and their amount based on Gibbs Free Energy minimization [25]. To calculate the necessary steam flow rate, the input mass of reactants used was the gas composition arriving from the gasifier and the temperature was set to 350 °C, that is the lowest operating temperature considered for the GCU.

The main gas composition from the gasifier was taken from computational fluid dynamics (CFD) simulations performed by BIOS applying in-house developed and experimentally validated models. Nearly steam-saturated air at 75 °C was used as gasifying agent, and two feedstocks, woodchips (moisture content 30% in weight) and straw pellets (moisture content 8% in weight), were studied [26–29]. While the main gas composition was obtained from simulations, the amounts of tar, light condensable and volatile organic compounds were measured during test runs. More details on the measurement procedure are given in section 3.2.

The amounts of sulphur and chlorine in the biosyngas extracted with the slip stream were obtained from a mass balance. The inlet amount was measured with an ultimate analysis of the feedstock. The outlet amount was divided in three parts: one part in the gasifier ashes, one part in the flue gases from the gasifier, and one part in the slip stream biosyngas. The amounts in the ashes and in the flue gases were measured, while the amount in the slip stream biosyngas was obtained as difference. A sulphur content of 35.3 and 357.1 mg kg^{-1} humidified biosyngas was calculated for woodchips and straw pellets, respectively. Regarding chlorine, a concentration of 13.3 and 1618.2 mg kg^{-1} humidified biosyngas was calculated. High temperature sorbents able to remove the S and Cl compounds

present at equilibrium at 400 °C were selected from literature. The equilibrium concentrations of gaseous sulphur and chlorine compounds at the outlet of the GCU were calculated in the temperature interval 350–450 °C using 1 kg of biosyngas and 10 kg of the identified sorbents. The maximum temperature meeting the SOFC requirements was chosen as the GCU operating temperature.

3.2. Experimental data: tar sampling and analysis

To develop a system model as close as possible to the real system, an experimental campaigned was conducted to sample and analyse the quantity and the tar species generated in the updraft gasifier. This approach was deemed very important for the study since the heat required to reform tar is highly dependent on the amount and chemical composition of tar and this is strictly dependent on the biomass used, the type of gasifier and the operating conditions [30].

The gasifier was operated two days with woodchips and one day with straw pellets. While wet sampling was used to measure tar compounds, the amount of some light hydrocarbons (propene) and some light condensable species (formaldehyde, acetic acid, methanol and ethanol) were measured with Fourier-transform infrared spectroscopy (FT-IR). The sampling was performed following the tar protocol (CEN TC BT/TF 143 WI CSC 03002.4) [31]. The samples were analysed with gravimetric analysis in BIOS Bioenergiesysteme, Graz, and with gas chromatography mass spectrometry (GC-MS) analysis in Energy Research Center (ECN) of the Netherlands, Petten. In gravimetric analysis, the samples were evaporated for roughly 20 h at ambient pressure and 60 °C. An elemental analysis was done on the gravimetric tar to determine the weight fractions of carbon, oxygen, hydrogen and nitrogen. In GC-MS analysis, the GC oven was operated between 40 °C and 245 °C and ECN method B.C302 (suitable for pyrolysis oil type tar) was used. Gravimetric analysis gives the amount of condensable tar present in syngas but not their chemical composition. Moreover, during this analysis, some of the volatile organic and light condensable compounds are lost thus giving an incomplete picture of the biosyngas composition. Conversely, GC-MS analysis can measure light condensable and volatile organic compounds, and gives the amounts of single tar compounds present in the mixture. Unfortunately, GC-MS cannot detect very heavy tar (Class 1) which are complex poly aromatic hydrocarbons, or complex molecular structures similar to the one found in pyrolysis oil and often referred to as pyrolytic lignin. In this work, it was assumed that all the compounds present in gravimetric tar could be represented by a selection of a few representative primary tar compounds.

An empirical formula for gravimetric tar was calculated from the gravimetric tar elemental analysis. Two of the most abundant compounds from GC-MS analysis were selected and, together with a third compound selected among primary tar compounds reported in Ref. [30], their weight percentage in biosyngas was calculated to match with the empirical formula calculated. These three compounds were used to represent gravimetric tar. The compounds selected have boiling points at atmospheric pressure higher than 60 °C and vapour pressure at 25 °C lower than that of isopropanol. These constraints were chosen to avoid selecting compounds which are not actually present in gravimetric tar.

3.3. System modelling

A system model was created using the software Aspen Plus, as illustrated in Fig. 2.

In all the simulated cases, the fuel utilization and the electricity produced by the SOFC (SOFC-DC) remained constant and equal to 0.8 and 6 kW, and the biosyngas flowrate required (SLIP-GAS) was calculated accordingly. The biosyngas is assumed to be extracted from the gasifier at 440 °C, and is then humidified with superheated steam (SLIP-WT) at 260 °C. In the real system, the heat from the combustion of the remaining biosyngas is used to generate the required steam.

The HCl, H_2S and particulate matter removal stages of the GCU are modelled with two heat exchangers. The first accounts for the heat losses to the environment, and the second one for the heat transfer from the afterburner (AFTBRN) off gases. The heat losses are assumed equal to 400 W and were calculated from a preliminary coarse design of the gas cleaning unit based on previous experience in the "BioCellus" project [32]. The biosyngas leaves the GCU at 395 °C. In case A, biosyngas is heated up to 740 °C in the tar reformer (TAR-REF). At this operating temperature, tar components are expected to be reformed [33]. The tar reformer is modelled with a Gibbs reactor with heat losses to the environment equal to 160 W. Also in this case, the heat losses were assumed based on a preliminary coarse design of the component. In cases B and C, biosyngas enters the CPOX unit where it is partially combusted. The unit is modelled with a stoichiometric reactor with heat losses to the environment of 160 W assumed equal to those of the tar reformer. The air flow rate is calculated in order to reach a biosyngas temperature of 740 °C. In case D, biosyngas enters a heat exchanger (ANODE-HX) where it is heated up to a temperature of 740 °C by the afterburner off gases. Table 1 summarizes the four cases analysed.

The software Aspen Plus does not include an SOFC model. Therefore, the SOFC is modelled using four blocks: a Gibbs reactor (ANODE) that simulates the electrochemical reactions; a separator (CA-SEP) that separates the amount of oxygen ions crossing through the electrolyte; a heat exchanger (CA-HEAT) to calculate the amount of air required to maintain the SOFC temperature; and a splitter to split the electricity and heat losses from the total enthalpy variation in the anode reactor. In this SOFC model, the fuel utilization, cell active area and area specific resistance are given as input parameters. The heat losses of the SOFC (SOFC-HLS) are assumed equal to 900 W. The values were taken from the stack manufacturer and from previous experience of AVL. The equations used to model the SOFC and to perform the electrochemical calculations are presented in Appendix A.1. Air at 25 °C is preheated in a heat exchanger (AIR-HX) by the exhaust gases coming from the afterburner up to 700 °C before entering the SOFC. This value was obtained by simulations performed by AVL using suppliers data to model the heat exchanger.

The outlet flows from the SOFC are fed into the afterburner, modelled with a stoichiometric reactor with heat losses of 220 W. The afterburner off gases are then separated: one part is used to heat the cathode air and the other part is used for biosyngas heat requirements. The two streams are then merged again before being fed to the heat recovery section (HT-RECOV) where hot water at 80 °C is produced. The exhaust flow at 84 °C is finally compressed in a blower (SOFC-CMP) and discarded to the environment at 133 °C (SOFC-FG).

A power electronics unit is used to condition the electricity produced in the SOFC (W-CDTNR). This unit is composed of two components: a DC/DC rectifier and a DC/AC converter. Part of the electricity (W-COMP) is supplied to the SOFC blower, part is lost due to conversion losses (EL-LOSS), and the remaining is converted into useful AC power (W-NET). Table 2 summarizes the input values used in the model. Where not previously specified, values were taken from prior experience of project partners.

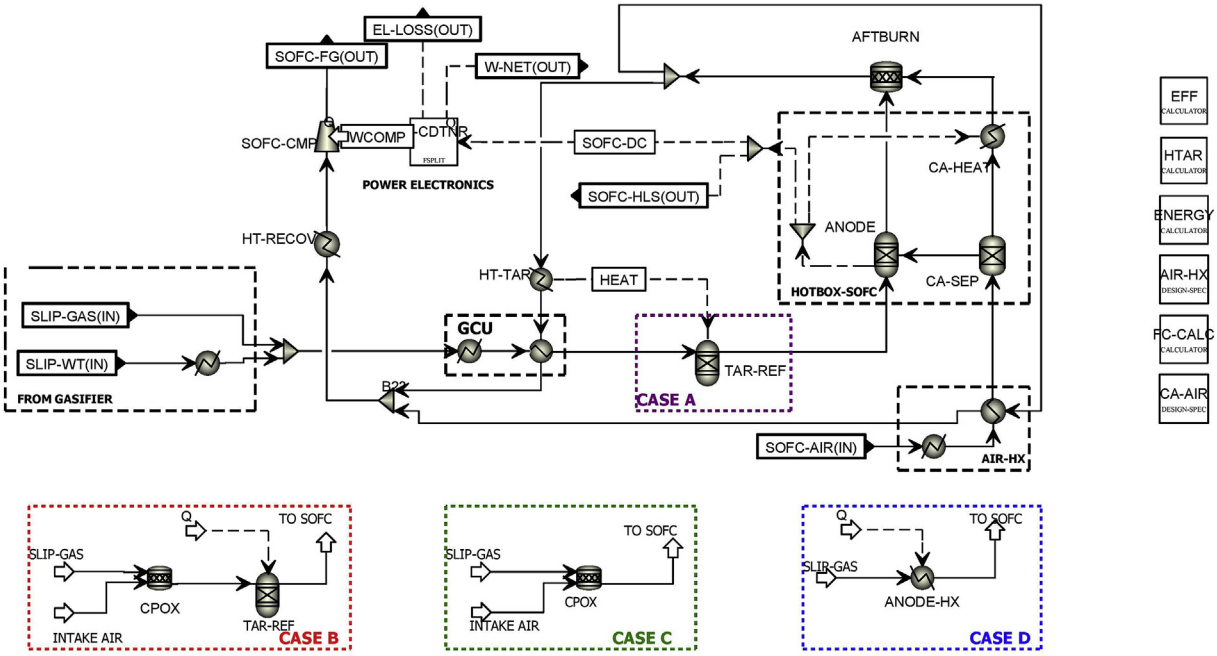

Fig. 2. Aspen flowsheet of the four system configurations analysed.

Table 1
System configurations analysed.

		Heating up strategy	
		afterburner off gases	*CPOX*
Reforming strategy	*External*	Case A	Case B
	Internal	Case D	Case C

4. Results

4.1. Thermodynamic equilibrium calculations

Equilibrium calculation showed that at 350 °C, which is the lowest temperature considered for the GCU operation, the steam amount necessary to avoid carbon formation is 0.12 and 0.25 kg per kg of biosyngas in case of woodchips and straw pellets, respectively. Table 3 presents the gas composition after the steam addition.

The calculations also showed that at 400 °C, S and Cl are mostly present as HCl, H_2S, and to a minor extent as COS, as shown in Table 4, where the contaminants concentrations are reported. For both feedstock, the concentration of contaminants in biosyngas is above the SOFC thresholds of 1 ppmv for H_2S and 5 ppmv for HCl. The biosyngas derived from straw pellets contains a significantly higher concentration of HCl (two orders of magnitude) and also of H_2S (one order of magnitude).

Alkaline earth and alkali metal-based sorbents can be used to decrease the concentration of HCl [35]. The reactions are illustrated as follows:

$$2HCl_{(g)} + 2NaAlO_{2(s)} \rightarrow 2NaCl_{(s)} + Al_2O_{3(s)} + H_2O_{(g)} \quad (4)$$

$$2HCl + Na_2CO_3 \rightarrow 2NaCl + CO_2 + H_2O \quad (5)$$

Potassium compounds are capable of achieving lower residual HCl concentrations as compared to sodium compounds. However, the vapour pressure of KCl is higher than that of NaCl, the two products of the cleaning reactions [36]. Nonetheless, potassium carbonate was selected as sorbent for HCl removal since the operating temperature is too low to result in relevant concentrations of gaseous KCl. The equilibrium HCl concentration is roughly two orders of magnitude lower than the limit value in the whole temperature range (see Table 5). The results are in agreement with the calculations and experiments performed by Krishnan et al. [36,38].

Metal based sorbents, such as zinc or copper oxides are a good option for H_2S removal from biosyngas, according to reactions (6) and (7) [35]. Moreover, carbonyl sulfide might be also directly removed by these sorbents, or it can be converted to H_2S in the GCU according to the hydrolysis reaction (8) [34].

$$H_2S_{(g)} + ZnO_{(s)} \rightarrow ZnS_{(s)} + H_2O_{(g)} \quad (6)$$

$$H_2S_{(g)} + CuO_{(s)} \rightarrow CuS_{(s)} + H_2O_{(g)} \quad (7)$$

$$COS(g) + H_2O(g) \rightarrow H_2S(g) + CO_2 \quad (8)$$

ZnO was selected as sorbent for H_2S removal although in reducing environments ZnO can be reduced to Zn and this might evaporate. Table 6 presents the residual concentrations of H_2S, COS an Zn as a function of sorbent temperature. Above 400 °C, H_2S concentration is very close to the target value of 1 ppmv. Despite thermodynamic equilibrium results suggest an operating temperature up to around 400 °C, Tamhankar et al. showed that experimentally H_2S concentration can be lowered below the expected equilibrium concentration due to the formation of a sulfide layer on the surface with free energy lower than the bulk sulphide [37]. The concentration of COS drops significantly below the ppmv value, and it is even lower than the ppbv value below 400 °C. The concentration of gaseous Zn results 1.61 ppbv at 450 °C and below the ppbv threshold at lower temperatures. Therefore, in this work the evaporation of zinc was not considered a threat for the system.

Although HCl concentration could be decreased well below the target value at temperatures higher than 400 °C, ZnO should not be operated above this temperature. Therefore, the GCU operating temperature was fixed at 400 °C. The calculation also showed that

Table 2
Model input parameters.

Inlet Flows		
Biosyngas temperature (SLIP-GAS)	440	[°C]
Steam temperature (SLIP-WT)	260	[°C]
SOFC air temperature (SOFC-AIR)	25	[°C]
Gas Cleaning Unit (GCU)		
Outlet syngas temperature	395	[°C]
Heat losses	400	[W]
Tar reformer (TAR-REF)		
Reactor temperature	740	[°C]
Heat losses	160	[W]
Heat exchanger (ANODE-HX)		
Heat losses	160	[W]
CPOX unit		
Heat losses	160	[W]
SOFC unit		
Fuel utilization (based on SLIP-GAS)	0.8	
Cell active area	127	[cm^2]
Area specific resistance	0.35	[$\Omega\ cm^2$]
Outflows temperature	830	[°C]
SOFC reaction temperature	830	[°C]
DC power	6000	[W]
Heat losses	900	[W]
Air heat exchanger (AIR-HX)		
Air outlet temperature	700	[°C]
Flue gas outlet temperature	180	[°C]
Heat losses	160	[W]
Power electronics (W-CDTNR)		
Electric efficiency	95	[%]
After burner (AFTBURN)		
Heat losses	220	[W]
Heat recovery unit (HT-RECOV)		
Heat losses	160	[W]
SOFC compressor (SOFC-CMP)		
Isentropic efficiency	70	[%]
Electric efficiency	95	[%]
Others		
Pressure drop in components	1	[%]

Table 3
Gas composition after slip stream humidification.

Compound	Woodchips	Straw pellets
	[wt% w.b.]	[wt% w.b.]
CO	12.01	10.10
H_2O	33.33	33.53
CO_2	15.15	15.53
H_2	0.92	0.80
CH_4	0.67	0.68
C_2H_4	0.62	0.62
gravimetric tar	4.80	5.80
formaldehyde	0.31	0.37
propene	0.43	0.52
acetic acid	1.72	2.08
methanol	0.12	0.15
ethanol	0.74	0.89
N_2	29.18	28.93

HCl reacts with ZnO forming $ZnCl_2$. This does not affect the removal of H_2S and COS but the equilibrium concentration of gaseous $ZnCl_2$ is between 2.5 and 5.3 ppmv in the temperature interval under analysis. This compound might damage the SOFC. Moreover, at 300 and 325 °C liquid $ZnCl_2$ might form. Conversely, S compounds do not react with K_2CO_3. Therefore, HCl removal should be carried out before that of H_2S.

Table 4
Equilibrium sulphur and chlorine compounds concentrations at 400 °C.

Species	molar fraction
Woodchips	
HCl	8.1E-06
H_2S	2.4E-05
COS	3.5E-08
Straw pellets	
HCl	8.7E-04
H_2S	2.1E-04
COS	3.2E-07

Table 5
Influence of temperature on HCl removal with K_2CO_3.

Temperature [°C]	HCl molar fraction
350	1.5E-09
375	2.8E-09
400	5.1E-09
425	8.9E-09
450	1.5E-08

Table 6
Influence of temperature on H_2S removal with ZnO.

Temperature [°C]	H_2S molar fraction	COS molar fraction	Zn molar fraction
350	2.2E-07	below ppb	below ppb
375	3.8E-07	below ppb	below ppb
400	6.2E-07	below ppb	below ppb
425	9.6E-07	1.9E-09	below ppb
450	1.4E-06	3.6E-09	1.6E-09

4.2. Tar sampling and analysis

Gravimetric analysis indicated a tar amount of 120–130 g Nm^{-3} dry biosyngas for woodchips and 190 g Nm^{-3} for straw pellets. The results of the GC-MS analysis are reported in Fig. 3, where only the compounds with a concentration higher than 1 g Nm^{-3} dry biosyngas are presented. Some of the GC-MS measured compounds, such as acetic acid and methanol, were already included in biosyngas composition since they were measured with FT-IR, as explained in the methodology. The sum of all the species analysed was equal to 100–110 g Nm^{-3} of biosyngas for woodchips and 245 g Nm^{-3} for straw pellets. These amounts are different from the one measured with the gravimetric analysis. Gravimetric tar from straw pellets was less than the GC-MS measured tar, while for woodchips the opposite was observed (Fig. 4). This might be due to the lower moisture content of the fuel, 8 wt% as compared to 30 wt% for woodchips. Less water in the fuel resulted in higher fuel bed temperature in the gasifier. As a consequence, more pyrolytic lignin was converted into volatile organic compounds, which are detectable with GC-MS but not with gravimetric analysis.

Table 7 presents the gravimetric tar elemental composition. The large amount of oxygen indicates that the mixture was mostly composed of oxygenated compounds, in agreement with what reported in literature for updraft gasifiers and with the results of the GC-MS analysis [30,39].

The weight percentages were converted into number of moles and an empirical formula for gravimetric tar was calculated. The presence of nitrogen was considered negligible. Gravimetric tar was represented with the molecule $C_{4.89}H_{6.25}O_{2.18}$ for woodchips and $C_{4.73}H_{6.35}O_{2.31}$ for straw pellets. Three compounds were selected and their ration was calculated to match the empirical formula. The compounds selected to represent gravimetric tar are 2-methoxyphenol, hydroxyaceton and hydroxyacetic acid. While the first two compounds were measured with the GC-MS analysis, the last compound was selected to close the elemental mass balance from a list of primary tar reported in Ref. [30]. Table 8 reports the weight percentages of the selected tar compounds in the humidified biosyngas.

The compounds selected are representative of both the carbohydrate-derived and lignin-derived part of the feedstock [40,41]. The three compounds have boiling point well above 60 °C, that is the temperature used in the gravimetric analysis. Moreover, their vapour pressure is significantly lower than that of isopropanol and acetic acid, as visible from the values reported in Table 9. Therefore, they were assumed to remain in the gravimetric sample. Analysis with GC-MS of the gravimetric residue dissolved in isopropanol could give an indication of the accuracy of this

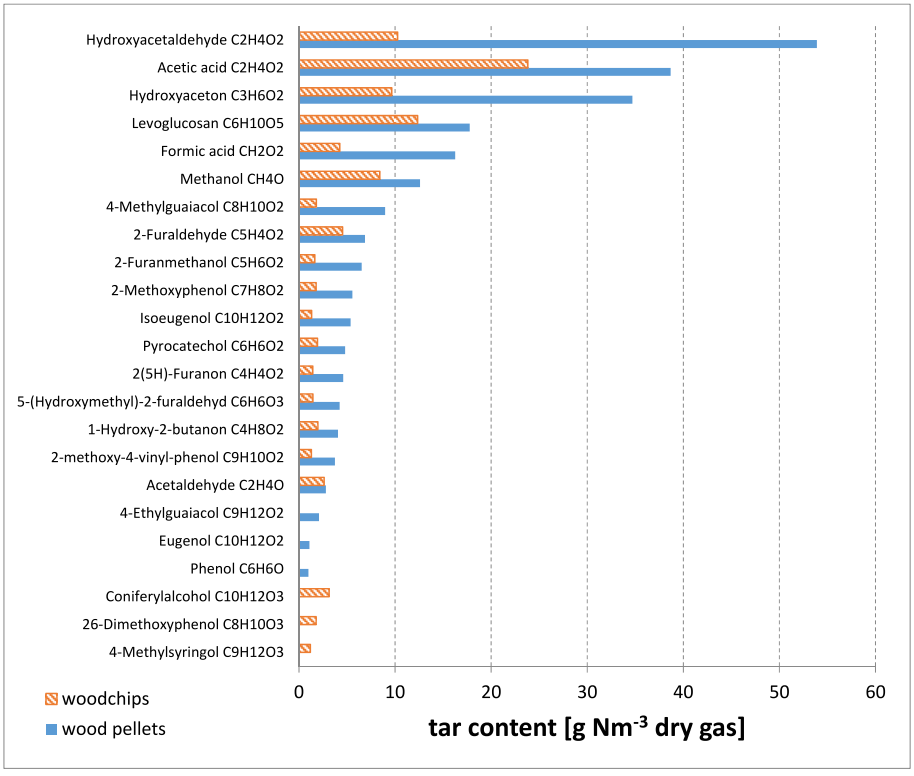

Fig. 3. GC-MS analysis results for woodchips (dashed) and straw pellets (solid).

Fig. 4. Comparison of gravimetric (dashed) and GC-MS (solid) analysis.

Table 7
Gravimetric tar elemental composition.

Element	Woodchips [wt% w.b.]	Straw pellets [wt% w.b.]
C	58.70	56.90
H	6.30	6.50
O	34.90	36.60
N	0.16	0.10

Table 9
Boiling temperature and vapour pressure at 25 °C of the selected compounds.

Compound	Boiling Temperature [°C]	Vapour pressure [mm Hg]
Isopropanol	83	45.4
Acetic acid	118	15.7
Hydroxyaceton	145	2.95
2-methoxyphenol	205	0.103
Hydroxyacetic acid	100	0.0202

assumption.

4.3. System modelling

The first results of the modelling activities are the SOFC operating conditions, as illustrated in Fig. 5. There is no significant difference in operating conditions between the two fuels in analysis. Similarly, the option for internal or external reforming (case D,C vs case A,B) has negligible impact on the operating conditions of the fuel cell. Conversely, substantial differences are visible depending on the biosyngas heating up strategy adopted (case A,D vs case B,C). Using the afterburner off gases results in higher reversible voltage and cell voltage. This is due to the higher H_2 concentration in the biosyngas reaching the anode.

The model was then used to calculate the flow rates necessary to generate 6 kW in the SOFC keeping the fuel utilization equal to 0.8. Table 10 illustrates the mass flow rates of biosyngas, steam, cathode air, and CPOX air. When part of the biosyngas is combusted in the CPOX unit (cases B and C), more biosyngas is necessary to generate the targeted 6 kW. As a consequence, also the flow rate of water to be added to the slip stream to avoid carbon deposition increases. In all the cases analysed, the biosyngas flow rate from straw pellets is lower than the one from woodchips. This result shows the importance of using the energy content of light condensable and volatile organic compounds, and gravimetric tar. In fact, straw pellets-derived biosyngas has a lower content of CO and almost equal content of H_2 and CH_4, but it has a larger content of these compounds. The data also show clearly the reduction in SOFC cooling needs due to direct internal tar reforming (cases C and D). In case of woodchips-derived biosyngas, the cathode air decreases from approximately 87 kg h^{-1} to 61 kg h^{-1} and in case of straw pellets-derived biosyngas, due to the larger tar content, the SOFC air reduces even further from around 87 kg h^{-1} to 57 kg h^{-1}.

The model was then used to compare the energy performances of the different system configurations. Table 11 shows the results of the system energy analysis. The required energy input varies between roughly 14 and 17 kW depending on the biosyngas heating-up strategy adopted, in accordance with the previously discussed larger biosyngas flowrate necessary to generate the target 6 kW in the SOFC when the CPOX unit is used. In the system, between 4 and 6 kW are lost. The two cases with external reformer are the ones with the largest total energy losses, equal to 5.3 kW and 5.7 kW when the afterburner off gases and the CPOX unit are used to heat up the biosyngas, respectively. The reason for this behaviour can be

Table 8
Amount of the selected representative tar in the humidified biosyngas.

Compound		Woodchips [wt% w.b.]	Straw pellets [wt% w.b.]
2-Methoxyphenol	$C_7H_8O_2$	3.51	3.63
hydroxyacetic acid	$C_2H_4O_3$	1.07	1.26
Hydroxyaceton	$C_3H_6O_2$	0.22	0.91

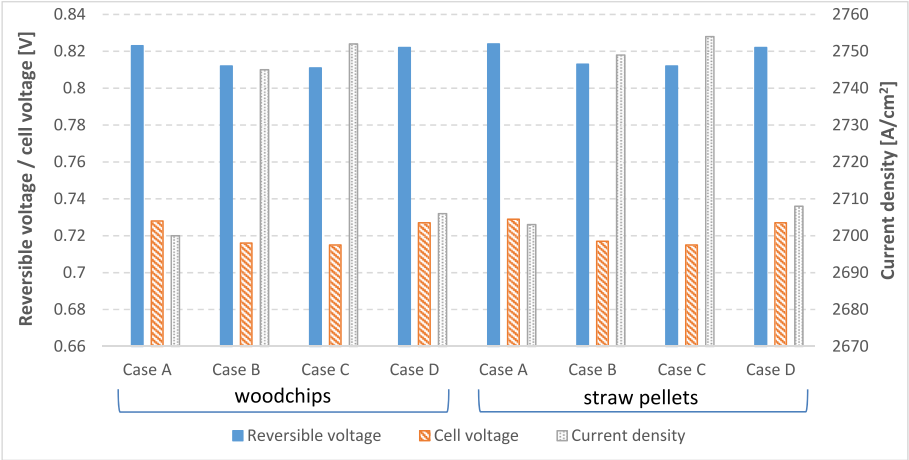

Fig. 5. SOFC operating results.

Table 10
Biosyngas, steam, cathode air and, CPOX air mass flow rates.

Case		Woodchips				Straw pellets			
		A	B	C	D	A	B	C	D
Mas flow rate [kg h^{-1}]	SLIP-GAS	8.46	10.42	10.45	8.48	7.38	9.08	9.11	7.39
	SLIP-WT	1.02	1.25	1.25	1.02	1.84	2.27	2.28	1.85
	Int. air (CPOX)	–	2.92	2.90	–	–	2.88	2.89	–
	SOFC-Air	86.85	86.66	60.9	61.29	86.82	86.70	56.49	56.89

Table 11
Results of system energy analysis.

		Woodchips				Straw pellets			
		A	B	C	D	A	B	C	D
Energy input [kW]	SLIP-GAS	13.75	17	17.25	13.82	13.46	16.57	16.62	13.49
	SLIP-WT	0.13	0.16	0.16	0.13	0.23	0.29	0.29	0.23
	Total	13.88	17.16	17.31	13.95	13.69	16.86	16.91	13.72
Energy losses [kW]	SOFC	0.9	0.9	0.9	0.9	0.9	0.9	0.9	0.9
	Other reactors	1.1	1.26	1.1	1.1	1.1	1.26	1.1	1.1
	DC/AC	0.3	0.3	0.3	0.3	0.3	0.3	0.3	0.3
	Chimney	3.04	3.23	2.3	2.3	3.03	3.21	2.28	2.12
	Total	5.34	5.69	4.6	4.6	5.33	5.67	4.58	4.12
Energy transmitted [kW]	SOFC-CMP	0.55	0.58	0.41	0.41	0.55	0.58	0.41	0.38
Energy output [kW]	W-NET	5.15	5.12	5.29	5.29	5.15	5.12	5.29	5.32
	HT-RECOVER	3.69	6.26	7.49	4.36	3.48	6.38	7.35	4.06
	Total	8.84	11.77	12.61	9.65	8.63	11.5	12.64	9.38

ascribed to the higher chimney losses that are higher when external reformer is used since a larger cathode air flow rate is necessary to maintain the SOFC operating temperature. The energy losses at the chimney, equal to around 3 kW in case of external reformer and 2 kW in the configuration with direct internal reforming, account for the largest losses, as visible in Fig. 6, where the share of the losses in the configuration with direct internal reforming and afterburner off gases utilization (case D) is presented for woodchips-derived biosyngas. On top of decreasing the chimney energy losses, the lower cathode flow rate achievable with direct internal reforming results also in lower energy required by the SOFC compressor, that decreases from 0.6 to 0.4 kW with both fuels and in both CPOX and afterburner off gases configurations. As a consequence, the net energy output also increases marginally. Using the CPOX unit results in slightly higher losses due to the presence of an additional component, thus an increased heat loss; moreover, the higher biosyngas flow rate required to produce the

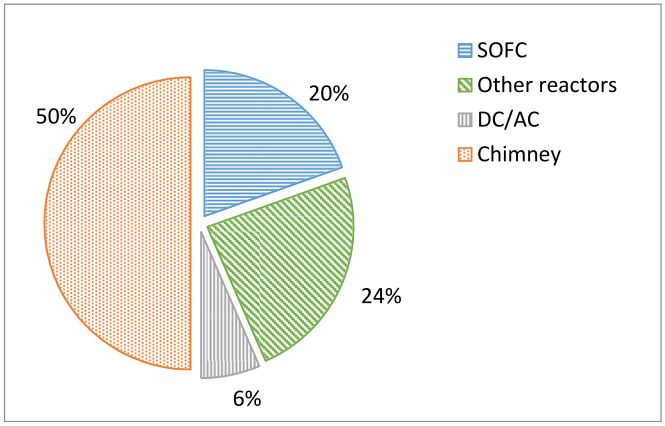

Fig. 6. Energy losses in the system (case D) fed with woodchips.

target 6 kW and the additional presence of 2.9 kg h^{-1} air for the CPOX operation further increase the chimney losses. The choice between using the afterburner off gases or the CPOX unit significantly affects also the amount of heat available in the recovery section. In case of woodchips as fuel, the heat recovered decreases when using the afterburner off gases from 6.3 kW to 3.7 kW with external reforming, and from 7.5 kW to 4.4 kW with direct internal reforming. The same trend holds true for pellet as fuel. Using the afterburner off gases to heat up the biosyngas and to sustain the reforming reactions in the external reformer (case A) results in the lowest amount of heat available, equal to 3.5 kW with straw pellets-derived biosyngas. Although to a minor extent, also the reforming strategy affects the heat that can be recovered, that increases from 3.7 kW to 4.4 kW for woodchips and from 3.5 kW to 4.0 kW for straw pellets in the configuration with after burner off gases utilization.

Fig. 7 shows the electrical, thermal, and total efficiency achievable with woodchips- and straw pellets-derived biosyngas in the different system configurations. The equations used to calculate the efficiencies can be found in Appendix A.2. The highest overall efficiency, that is 74% with woodchips and 75% with straw pellets, is achieved with direct internal tar reforming and using the CPOX unit to increase the biosyngas temperature before the SOFC. Using the CPOX unit results in higher overall efficiencies due to an increase in the thermal efficiency. However, it significantly lowers the system electrical efficiency to around 30% as compared to roughly 37% achievable when the afterburner off gases are used to heat up the biosyngas. Fuel cells are electrochemical devices and therefore to achieve high voltages and efficiencies, it is important to keep high the chemical energy of the fuel before it enters the fuel cell. The lower cathode air required due to direct internal reforming slightly reduces the electricity consumption by the compressor and the system electrical efficiency increases from 37.1% to 38.0% with woodchips as fuel and from 37.6% to 38.8% with straw pellets in the configurations with the afterburner off gases to heat up the biosyngas. In the configuration with the CPOX unit, direct internal reforming increases the system electrical efficiency from 30.4% to 31.3% with pellets and 29.9%–30.6% with woodchips. Direct internal reforming also increases the system thermal efficiency thanks to the higher amount of heat available in the recovery section and the lower heat depleted through the chimney thanks to the decreased cathode flow.

The results obtained in the energy analysis are also presented in the form of energy flows. Fig. 8 illustrates the two cases with external reformer and woodchips as fuel. Focusing on the amount of chemical energy and thermo-mechanical energy, it can be seen that for case A, there is an increase in chemical energy of the fuel flow that exits the tar reformer . The reforming reactions produce additional chemical energy with the help of the thermo-mechanical energy provided by the afterburner off gases. On the other hand, when the CPOX unit is employed as in case B, a part of the chemical energy is converted into thermo-mechanical energy when the gas passes through the CPOX unit . Considering that the slip stream extraction is used for electricity production, it might appear reasonable to design the system to have the highest electrical efficiency, that is using the afterburner off gases to heat up the biosyngas.

The efficiency results obtained from the system modelling can be compared with the results achieved with the real system during the Horizon2020 project “FlexiFuel-SOFC”. These results are not used as validation of the model, but rather as additional information on the performance that can be actually achieved with an integrated biomass gasifier SOFC CHP system. The configuration of the real system is slightly different from the one adopted in the model since, after having gained experience with a first pilot plant, a second improved pilot plant was built. Moreover, as initially mentioned, the model does not include the gasifier, but it starts from the slip stream and it ends with the boiler, where only the afterburner off gases are used to generate heat. Therefore, the energy input in the model is the biosyngas extracted in the slip stream, while in the real system it is the solid biomass fed to the gasifier. Furthermore, in the real system the biosyngas that is not extracted with the slip stream is used to generate additional heat. Last, despite the successful operation of SOFC with tar-containing biosyngas, since there is not yet general agreement on the fate of tar in the anode chamber, in the system tar was converted before reaching the SOFC [42]. A total efficiency of 80% was achieved with the real system and this can be further increased to 91% by adopting a condenser in the heat recovery section. The SOFC used the biosyngas to generate electricity with a gross DC efficiency higher than 42%, and the heat recovered from the SOFC exhaust accounted for 21% of the total system energy output. The project results have been

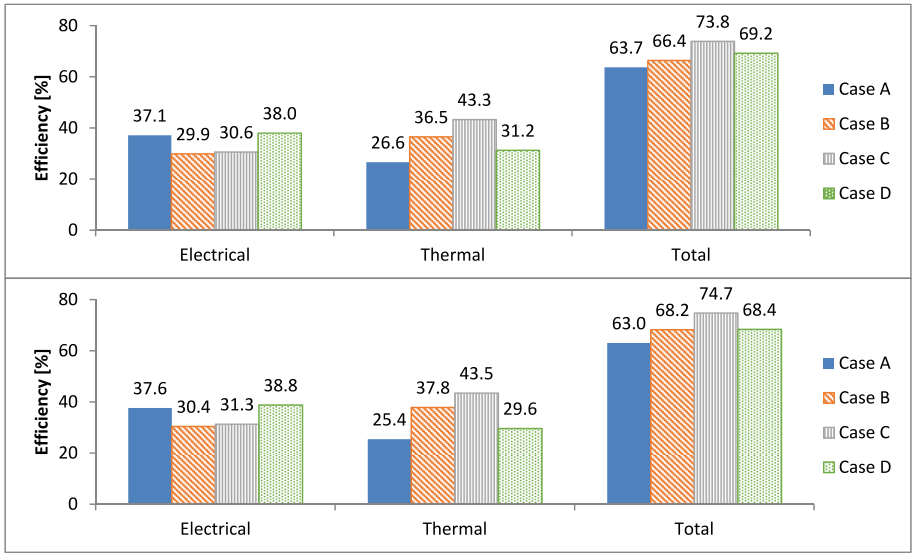

Fig. 7. Electrical, thermal, and total efficiency with (top) woodchips- and (bottom) straw pellets-derived biosyngas.

Case A

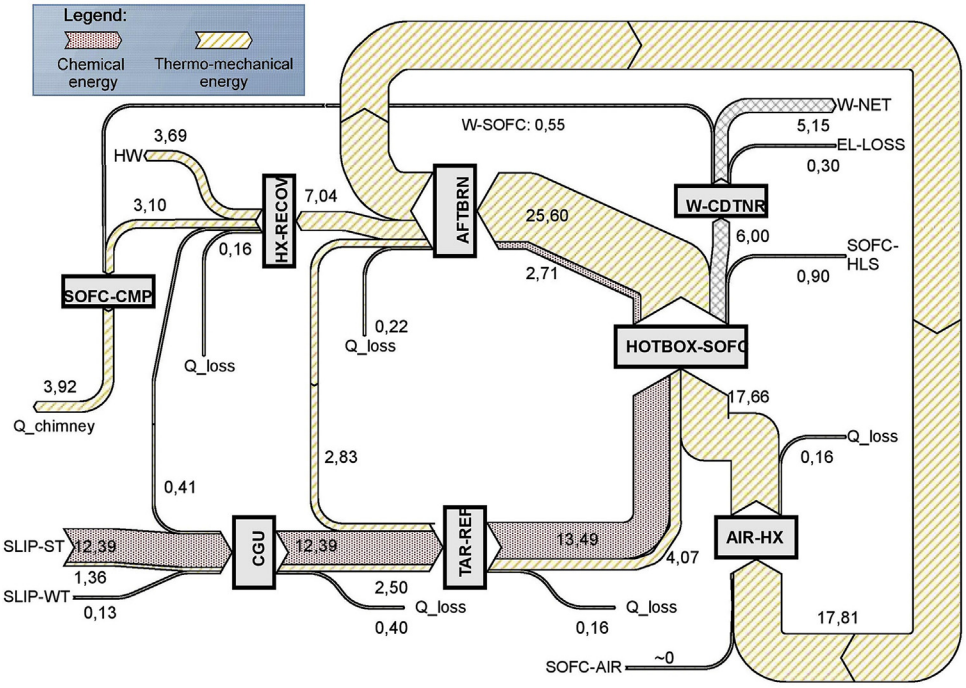

Case B

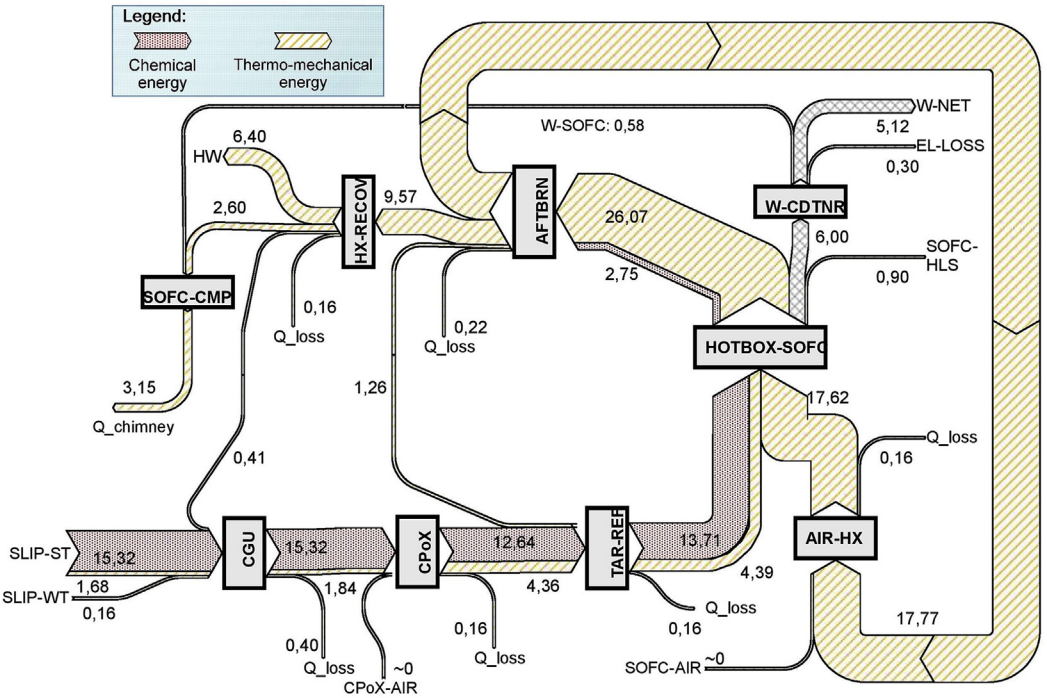

Fig. 8. Energy flows of the two system configurations with external reformer and woodchips as fuel.

presented during the final project workshop held during the European Biomass Conference and Exhibition (EUBCE) 2019 in Lisbon. More details can be found on the project website flexifuelsofc.eu, where the presentations given in the workshop are available for download [43].

The model developed in this study will be further improved in our future work. The gasification step will be included and the system configuration will be revised to represent the final "FlexiFuel-SOFC" system design. Moreover, the values used in terms of pressure drops and heat losses will be updated in light of the measurement performed with the real system. The model will be successively validated thanks to the results of the extensive experimental campaign carried out within the project.

5. Conclusion

This work aimed to improve the competitiveness of an integrated biomass updraft gasifier SOFC micro CHP system. This was done by increasing system efficiency and reducing its complexity via direct internal reforming of hydrocarbons. We used a comprehensive approach combining system modelling, thermodynamic equilibrium calculations and experimental data to evaluate the efficiency gain obtainable, identify an appropriate gas cleaning configuration, and compare two strategies to heat up the biosyngas before feeding it to the SOFC: catalytic partial oxidation and afterburner off gases utilization.

The GCU has to operate at temperatures lower than 400 °C to decrease H_2S and HCl below SOFC tolerance limit using ZnO and K_2CO_3 as sorbents. However, HCl removal should be carried out before that of H_2S to avoid reactions between ZnO and HCl leading to the formation of $ZnCl_2$. Gravimetric analysis indicated a tar amount of 120–130 g Nm^{-3} dry biosyngas for woodchips and 190 g Nm^{-3} for straw pellets. Differently, the sum of all the species analysed with GC-MS analysis was equal to 100–110 g Nm^{-3} dry biosyngas for woodchips and 245 g Nm^{-3} for straw pellets. The majority of the tar measured with GC-MS analysis belongs to the primary tar group, and 2-methoxyphenol, hydroxyacetic acid and hydroxyacetone were selected as representative compounds.

Direct internal tar reforming reduces the SOFC cooling needs. In case of woodchips-derived biosyngas, the cathode air decreases from approximately 87 kg h^{-1} to 61 kg h^{-1} and from around 87 kg h^{-1} to 57 kg h^{-1} in case of straw pellets-derived biosyngas. The lower cathode air required due to direct internal reforming reduces the electricity consumption by the compressor and the system electrical efficiency increases from 37.1% to 38.0% with woodchips as fuel and from 37.6% to 38.8% with straw pellets in the configuration with the afterburner off gases used to heat up the biosyngas. In the configuration with the CPOX unit, direct internal reforming increases the system electrical efficiency from 30.4% to 31.3% with pellets and 29.9%–30.6% with woodchips. When tar is reformed internally also the heat that can be recovered increases.

Using the CPOX unit results in higher overall efficiencies due to an increase in the thermal efficiency. The heat recovered increases when using the CPOX unit. However, it significantly lowers the system electrical efficiency to around 30% as compared to roughly 38% achievable when the afterburner off gases are used to heat up the biosyngas. Since the system is used for electricity production, it is reasonable to adopt the configuration with the highest electrical efficiency, that is with after burner off gases utilization.

A simplified system design can be obtained with direct internal reforming, which might also have a significant impact on both capital and operation costs of the system. A techno-economic analysis can be used to evaluate the advantages at system level. From an energy point of view, direct internal reforming brings an increase in electrical efficiency of around 1% point and in thermal efficiency of even 5–6% points. The choice of direct internal tar reforming seems therefore an advantageous strategy to improve the competitiveness of an integrated biomass updraft gasifier SOFC micro CHP system.

Declaration of competing interest

The authors declare that they have no known competing financial interests or personal relationships that could have appeared to influence the work reported in this paper.

Acknowledgement

This research is partially supported by the project "FlexiFuel-SOFC". The project has received funding from the European Union's Horizon 2020 research and innovation programme under grant agreement No. 641229.

Appendix A. Thermodynamic approach

A.1 SOFC modelling

Aspen plus is not provided with an SOFC model. Therefore, a combination of various blocks and a fortran-based code written in a calculator block is needed for SOFC modelling and to perform the electrochemical calculations.

The reversible voltage (E_{rev}) is calculated as:

$$E_{rev} = \frac{R \cdot T_{SOFC}}{4 \cdot F} \cdot \ln\left(\frac{p_{O_2,cathode}}{p_{O_2,anode}}\right) \quad (1)$$

$E_{rev} = \frac{R \cdot T_{SOFC}}{4 \cdot F} \cdot \ln\left(\frac{p_{O_2,cathode}}{p_{O_2,anode}}\right)$ where R is the ideal gas constant (J/kg.mol), T_{SOFC} is the operating temperature of the fuel cell (K), p is the partial pressure of the oxygen in the anode and cathode sides (Pa) and F is the Faraday's constant (C/mol) [44].

The cell voltage (V_{cell}) is determined as:

$$V_{cell} = E_{rev} - j \cdot ASR \quad (2)$$

$V_{cell} = E_{rev} - j \cdot ASR$

Being j is the current density (A/m^2) and ASR is the area-specific resistance ($\Omega.m^2$) [45].

The biosyngas flow rate is calculated by determining the equivalent H_2 content of the anode inlet flow. The equivalent H_2 content is given by the content of hydrogen available after complete reforming and water gas shift of the hydrocarbons.

A.2 Efficiency calculations

The electric efficiency is calculated as

$$\eta_{electric} = \frac{\dot{W}_{SOFC} - \dot{W}_{DC/AC} - \dot{W}_{SOFC-CMP}}{\dot{m}_{SLIP-ST} \cdot (LHV + \Delta h) + \dot{m}_{SLIP-WT} \cdot \Delta h} \quad (3)$$

$\eta_{electric} = \frac{\dot{W}_{SOFC} - \dot{W}_{DC/AC} - \dot{W}_{SOFC-CMP}}{\dot{m}_{SLIP-ST} \cdot (LHV + \Delta h) + \dot{m}_{SLIP-WT} \cdot \Delta h}$ The energy of biosyngas (SLIP-ST) is given by the lower heating value (LHV in kJ/mol) added to the enthalpy variation (Δh in kJ/kg) from 25 °C to 440 °C multiplied by its mass flow (kg/s). To remark that, from the enthalpy variation calculation for both biosyngas and steam (SLIP-WT), the latent heat of water is subtracted. The net electricity ($\dot{W}_{NET}$ in kW) is given by the SOFC electricity production ($\dot{W}_{SOFC}$)

subtracted by the electric losses in the power electronics ($\dot{W}_{DC/AC}$) and the electricity supplied to the compressor ($\dot{W}_{SOFC-CMP}$).

The thermal efficiency is calculated as

$$\eta_{thermal} = \frac{\dot{Q}_{HT-RECOV}}{\dot{m}_{SLIP-ST} \cdot (LHV + \Delta h) + \dot{m}_{SLIP-WT} \cdot \Delta h} \quad (4)$$

$\eta_{thermal} = \frac{\dot{Q}_{HT-RECOV}}{\dot{m}_{SLIP-ST} \cdot (LHV + \Delta h) + \dot{m}_{SLIP-WT} \cdot \Delta h} Q_{HT-RECOV}$ (kW) represents the heat transferred to the domestic hot water in the heat recovery section [46].

The total efficiency (η_{total}) of the system is calculated as

$$\eta_{total} = \eta_{electric} + \eta_{thermal}$$

Credit author statement

A. Cavalli: Conceptualization, Methodology, Experiments, Modelling, Visualization, Writing – review & editing. A. Fernandes: Conceptualization, Modelling, Writing, Reviewing, Visualization. P. V. Aravind: Supervision, Reviewing.

References

[1] Bang-Møller C, Rokni M, Elmegaard B, Ahrenfeldt J, Henriksen UB. Decentralized combined heat and power production by two-stage biomass gasification and solid oxide fuel cells. Energy 2013;58:527–37. https://doi.org/10.1016/j.energy.2013.06.046.

[2] Baldinelli A, Barelli L, Bidini G. Performance characterization and modelling of syngas-fed SOFCs (solid oxide fuel cells) varying fuel composition. Energy 2015;90:2070–84. https://doi.org/10.1016/j.energy.2015.07.126.

[3] Shayan E, Zare V, Mirzaee I. On the use of different gasification agents in a biomass fueled SOFC by integrated gasifier: a comparative exergo-economic evaluation and optimization. Energy 2019;171:1126–38. https://doi.org/10.1016/j.energy.2019.01.095.

[4] Gadsbøll RØ, Thomsen J, Bang-Møller C, Ahrenfeldt J, Henriksen UB. Solid oxide fuel cells powered by biomass gasification for high efficiency power generation. Energy 2017;131:198–206. https://doi.org/10.1016/j.energy.2017.05.044.

[5] Papurello D, Lanzini A, Drago D, Leone P, Santarelli M. Limiting factors for planar solid oxide fuel cells under different trace compound concentrations. Energy 2016;95:67–78. https://doi.org/10.1016/j.energy.2015.11.070.

[6] Bermudez JM, Fidalgo B. 15 - production of bio-syngas and bio-hydrogen via gasification. In: Luque R, Lin CSK, Wilson K, editors. Clark JBT-H of BP. Second E. Woodhead Publishing; 2016. p. 431–94. https://doi.org/10.1016/B978-0-08-100455-5.00015-1.

[7] Omosun AO, Bauen A, Brandon NP, Adjiman CS, Hart D. Modelling system efficiencies and costs of two biomass-fuelled SOFC systems. J Power Sources 2004;131:96–106. https://doi.org/10.1016/j.jpowsour.2004.01.004.

[8] Aravind PV, Woudstra T, Woudstra N, Spliethoff H. Thermodynamic evaluation of small-scale systems with biomass gasifiers, solid oxide fuel cells with Ni/GDC anodes and gas turbines. J Power Sources 2009;190:461–75. https://doi.org/10.1016/j.jpowsour.2009.01.017.

[9] Toonssen R, Sollai S, Aravind PV, Woudstra N, Verkooijen AHM. Alternative system designs of biomass gasification SOFC/GT hybrid systems. Int J Hydrogen Energy 2011;36:10414–25. https://doi.org/10.1016/j.ijhydene.2010.06.069.

[10] Liu M, Aravind PV, Woudstra T, Cobas VRM, Verkooijen AHM. Development of an integrated gasifier-solid oxide fuel cell test system: a detailed system study. J Power Sources 2011;196:7277–89. https://doi.org/10.1016/j.jpowsour.2011.02.065.

[11] Doherty W, Reynolds A, Kennedy D. Process simulation of biomass gasification integrated with a solid oxide fuel cell stack. J Power Sources 2015;277:292–303. https://doi.org/10.1016/j.jpowsour.2014.11.125.

[12] Wu Z, Zhu P, Yao J, Zhang S, Ren J, Yang F, et al. Combined biomass gasification, SOFC, IC engine, and waste heat recovery system for power and heat generation: energy, exergy, exergoeconomic, environmental (4E) evaluations. Appl Energy 2020;279:115794. https://doi.org/10.1016/j.apenergy.2020.115794.

[13] Detchusananard T, Sharma S, Maréchal F, Arpornwichanop A. Multi-objective optimization of sorption enhanced steam biomass gasification with solid oxide fuel cell. Energy Convers Manag 2019;182:412–29. https://doi.org/10.1016/j.enconman.2018.12.047.

[14] Roy D. Performance evaluation of a novel biomass-based hybrid energy system employing optimisation and multi-criteria decision-making techniques. Sustain Energy Technol Assessments 2020;42:100861. https://doi.org/10.1016/j.seta.2020.100861.

[15] Roy D, Samanta S, Ghosh S. Techno-economic and environmental analyses of a biomass based system employing solid oxide fuel cell, externally fired gas turbine and organic Rankine cycle. J Clean Prod 2019;225:36–57. https://doi.org/10.1016/j.jclepro.2019.03.261.

[16] Valderrama Rios ML, González AM, Lora EES, Almazán del Olmo OA. Reduction of tar generated during biomass gasification: a review. Biomass Bioenergy 2018;108:345–70. https://doi.org/10.1016/j.biombioe.2017.12.002.

[17] Basagiannis AC, Verykios XE. Steam reforming of the aqueous fraction of bio-oil over structured Ru/MgO/Al2O3 catalysts. Catal Today 2007;127:256–64. https://doi.org/10.1016/J.CATTOD.2007.03.025.

[18] Lanzini A, Kreutz TG, Martelli E, Santarelli M. Energy and economic performance of novel integrated gasifier fuel cell (IGFC) cycles with carbon capture. Int J Greenh Gas Control 2014;26:169–84. https://doi.org/10.1016/j.ijggc.2014.04.028.

[19] Nagel FP, Schildhauer TJ, Biollaz SMA. Biomass-integrated gasification fuel cell systems - Part 1: definition of systems and technical analysis. Int J Hydrogen Energy 2009;34:6809–25. https://doi.org/10.1016/j.ijhydene.2009.05.125.

[20] Nagel FP, Schildhauer TJ, McCaughey N, Biollaz SM a. Biomass-integrated gasification fuel cell systems – Part 2: economic analysis. Int J Hydrogen Energy 2009;34:6826–44. https://doi.org/10.1016/j.ijhydene.2009.05.139.

[21] Di Carlo A, Bocci E, Dell'Era A. Comparison by the use of numerical simulation of a MCFC-IR and a MCFC-ER when used with syngas obtained by atmospheric pressure biomass gasification. Int J Hydrogen Energy 2011;36:7976–84. https://doi.org/10.1016/j.ijhydene.2011.01.095.

[22] Rokni M. Biomass gasification integrated with a solid oxide fuel cell and Stirling engine. Energy 2014;77:6–18. https://doi.org/10.1016/j.energy.2014.01.078.

[23] Ud Din Z, Zainal ZA. Biomass integrated gasification-SOFC systems: technology overview. Renew Sustain Energy Rev 2016;53:1356–76. https://doi.org/10.1016/j.rser.2015.09.013.

[24] Ud Din Z, Zainal ZA. The fate of SOFC anodes under biomass producer gas contaminants. Renew Sustain Energy Rev 2016. https://doi.org/10.1016/j.rser.2016.10.012.

[25] Thermfact/CRCT, GTT-technologies. FactSage n.d. www.factsage.com.

[26] Brunner T, Ramerstorfer C, Obernberger I, Kerschbaum M, Aravind PV, Makkus R, et al. Development of a highly efficient micro-scale CHP system based on fuel-flexible gasification and a SOFC. In: 25th Eur. Biomass Conf. Exhib.; 2017. p. 725–31. https://doi.org/10.5071/25thEUBCE2017-2CV.3.5.

[27] Mandl C, Obernberger I, Biedermann F. Modelling of an updraft fixed-bed gasifier operated with softwood pellets. Fuel 2010;89:3795–806. https://doi.org/10.1016/j.fuel.2010.07.014.

[28] Mandl C, Obernberger I, Biedermann F. Updraft fixed-bed gasification of softwood pellets: mathematical modelling and comparison with experimental data. In: 17th Eur biomass Conf Exhib; 2009.

[29] Obernberger I, Brunner T, Mandl C, Kerschbaum M, Svetlik T. Strategies and technologies towards zero emission biomass combustion by primary measures. Energy Procedia 2017;120:681–8. https://doi.org/10.1016/j.egypro.2017.07.184.

[30] Milne TTA, Abatzoglou N, Evans RRJ. Biomass gasifier" tars": their nature, formation, and conversion, vol. 570; 1997. Colorado.

[31] Maniatis K, Beenackers AAC. Tar protocols. IEA bioenergy gasification task. Biomass Bioenergy 2000;18:2–5. https://doi.org/10.1016/s0961-9534(99)00072-0.

[32] Frank N, Saule M, Karl J. Final Report - BIOCELLUS (Biomass fuel cell utility system). 2011.

[33] Abdoulmoumine N, Adhikari S, Kulkarni A, Chattanathan S. A review on biomass gasification syngas cleanup. Appl Energy 2015;155:294–307. https://doi.org/10.1016/j.apenergy.2015.05.095.

[34] Andersen WC, Bruno TJ. Kinetics of carbonyl sulfide hydrolysis: 1. Catalyzed and uncatalyzed reactions in mixtures of water + propane. Ind Eng Chem Res 2003;42:963–70. https://doi.org/10.1021/ie020772z.

[35] Aravind PV, de Jong W. Evaluation of high temperature gas cleaning options for biomass gasification product gas for Solid Oxide Fuel Cells. Prog Energy Combust Sci 2012;38:737–64. https://doi.org/10.1016/j.pecs.2012.03.006.

[36] Krishnan GN, Canizales A, Gupta R, Ayala R. Development of disposable sorbents for chloride removal from high-temperature coal-derived gases. In: Adv. Coal-fired power Syst. '96 Rev. Meet. U.S. DOE, Morgantown Energy Technology Center; 1996.

[37] Tamhankar SS, Bagajewicz M, Gavalas GR, Sharma PK, Flytzani-Stephanopoulos M. Mixed-oxide sorbents for high-temperature removal of hydrogen sulfide. Ind Eng Chem Process Des Dev 1986;25:429–37. https://doi.org/10.1021/i200033a014.

[38] Krishnan GN, Gupta RP, Canizales A, Shelukar S, Ayala RE. Removal of hydrogen chloride from hot coal gas streams. High Temp Gas Clean 1996;1:405–14.

[39] Elliott DC. Relation of reaction time and temperature to chemical composition of pyrolysis oils. Pyrolysis oils from biomass, vol. 376. American Chemical Society; 1988. p. 6–55. https://doi.org/10.1021/bk-1988-0376.ch006.

[40] Wang D, Czernik S, Chornet E. Production of hydrogen from biomass by catalytic steam reforming of fast pyrolysis oils. Energy Fuels 1998;12:19–24. https://doi.org/10.1021/ef970102j.

[41] Peng C, Zhang G, Han J, Li X. Hydrothermal conversion of lignin and black liquor for phenolics with the aids of alkali and hydrogen donor. Carbon Resour Convers 2019;2:141–50. https://doi.org/10.1016/j.crcon.2019.06.004.

[42] Hofmann P, Panopoulos KD, Aravind PV, Siedlecki M, Schweiger A, Karl J, et al. Operation of solid oxide fuel cell on biomass product gas with tar levels >10 g Nm−3. Int J Hydrogen Energy 2009. https://doi.org/10.1016/j.ijhydene.2009.07.040. 34:9203−12.
[43] FlexiFuel-SOFC. n.d. http://www2.flexifuelsofc.eu/. [Accessed 5 May 2018].
[44] Williams M, Yamaji K, Horita T, Sakai N, Yokokawa H. Exergetic studies of intermediate-temperature, mixed ionic-electronic conducting solid oxide fuel cell electrolytes using the wagner mass transfer model. ECS Trans 2019;12: 303−15. https://doi.org/10.1149/1.2921556.
[45] DiGiuseppe G, Sun L. Electrochemical performance of a solid oxide fuel cell with an LSCF cathode under different oxygen concentrations. Int J Hydrogen Energy 2011;36:5076−87. https://doi.org/10.1016/j.ijhydene.2011.01.017.
[46] Pirkandi J, Penhani H, Maroufi A. Thermodynamic analysis of the performance of a hybrid system consisting of steam turbine, gas turbine and solid oxide fuel cell (SOFC-GT-ST). Energy Convers Manag 2020;213:112816. https://doi.org/10.1016/j.enconman.2020.112816.